Dynamic Compensation of Temperature Sensors Using a Continuum Model

Z.C. Feng and Yuwen Zhang
Department of Mechanical and Aerospace Engineering
University of Missouri
Columbia, MO 65211, USA
fengf@missouri.edu

Abstract—Most temperature sensors are known to have slow dynamic response. Dynamic compensation has been used to expand the sensor frequency bandwidth using the known sensor frequency responses. There has been extensive literature on the temperature sensor dynamic compensation using the first order model which ignores the heat conduction within the sensor itself. This paper proposes a continuum model that includes the heat conduction. The resulting mathematical model is analyzed using Laplace transform from which a non-polynomial transfer function is obtained. This non-polynomial transfer function is further used to obtain approximations that can be implemented in the time domain for sensor dynamic compensation. The effectiveness of the compensation is illustrated with the data obtained from numerical simulations for random sensor input.

Keywords—Sensor dynamic compensation, temperature sensor, bandwidth, sensor delay

I. INTRODUCTION

Measurement of fluctuating temperature is important in many engineering processes [1]. Temperature sensors based on various transduction principles have been used for many years. With rare exceptions [2], most temperature sensors are known to have slow time responses. In some applications such as the transport processes in turbulent combustion [3-4], the sensors are required to be accurate in measuring temperature fluctuations of up to 1000 Hz. There are also harsh measurement environment that requires protection to sensors which further add to the time lag in sensor response.

Methods for compensating slow sensors for fast measurements have been attracting increasing interests [5-13]. For temperature sensors specifically, earlier investigations focus on electrical techniques including RC circuits for differentiation [14]. A first order lumped capacitance model is widely used to characterize the frequency response of temperature sensors [15]. Compensation for the time lag can be achieved for known sensor time constant. However, in some applications, the sensor time constant can be spatially or temporally changing. Therefore, methods to obtain in situ sensor time constant have attracted extensive research interest [16-19].

The first order lumped capacitance model ignores the heat conduction within the sensor body. For many sensors with very small size, this assumption is reasonable and the resulting model is adequate. However, when measuring fast temperature fluctuations, the time constant characterizing the heat conduction within the sensor is no longer negligible. Furthermore, protective layers such as insulation coating over the sensor for use in harsh environment can render the model very inaccurate if the heat conduction is ignored [20-21].

When the sensor is treated as a continuum to include heat conduction, the governing equation becomes a partial differential equation. The sensor dynamic compensation becomes much more challenging. Sensor dynamic compensation has been carried out in the frequency domain using the known frequency responses of the sensor [22-23]. Although this method has been shown to be effective, it is based on the post processing of the acquired data. It is no-causal and cannot be implemented in real time. In this paper we develop an alternative that can be implemented in real time.

This paper treats the heat conduction problem on a spherical geometry with symmetry. In the following section, a transfer function is obtained using Laplace transform. The non-polynomial transfer function is used to illustrate the frequency response of the sensor obtained numerically in section 3. In section 4, approximations based on the Taylor series expansion of the transfer function are proposed to be used to dynamically compensate the sensor for applications to fast temperature fluctuations. In section 5, we use the sensor data obtained from numerical simulations corresponding to random sensor input to illustrate the effectiveness of the proposed method. Noises are also included in the simulations.

II. A CONTINUUM MODEL OF DYNAMIC RESPONSE OF A TEMPERATURE SENSOR

Consider a sensor with a spherical shape as shown in Figure 1. If the temperature inside the sphere, T_s is assumed to be uniform, we have the lumped capacitance model

$$\rho_s c_{ps} \frac{4\pi R^3}{3} \frac{dT_s}{dt} = 4\pi R^2 h(T_o - T_s) \qquad (1)$$

where ρ_s and c_{ps} are the density and specific heat of the solid respectively; they are assumed to be independent of temperature; h is the convective heat transfer coefficient and T_o is the temperature of the surrounding fluid. We call T_o the process temperature in the following. The first order equation can be written as

978-1-4673-8644-9/16/$31.00 ©2016 IEEE

$$\tau \frac{dT_s}{dt} + T_s = T_o, \tag{2}$$

where

$$\tau = \frac{\rho_s c_{ps} R}{3h} \tag{3}$$

is the time constant.

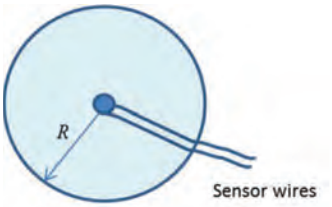

Figure 1 A model of a sensor with protection.

By assuming that the temperature inside the sphere be uniform, we obtain the so-called "first order lag" model involving only one parameter. Consider the geometry in Figure 1 where the sensing element is at the center of a finite size sphere. Assuming spherical symmetry, the temperature is governed by the heat conduction equation:

$$\rho_s c_{ps} \frac{\partial T_s}{\partial t} = \frac{k_s}{r^2} \frac{\partial}{\partial r}\left(r^2 \frac{\partial T_s}{\partial r}\right) \tag{4}$$

where k_s is the thermal conductivity and is assumed to be independent of temperature. This equation can be written as the standard one-dimensional heat equation:

$$\rho_s c_{ps} \frac{\partial (rT_s)}{\partial t} = k_s \frac{\partial^2 (rT_s)}{\partial r^2}. \tag{5}$$

The boundary condition on the spherical surface is that of convective boundary condition, i.e.

$$-k_s \left.\frac{\partial T_s}{\partial r}\right|_{r=R} = h(T_s|_{r=R} - T_o) \tag{6}$$

Equation (5) can be written as

$$\frac{t_c \partial (\tilde{r} T_s)}{\partial t} = \frac{\partial^2 (\tilde{r} T_s)}{\partial \tilde{r}^2} \tag{7}$$

where

$$t_c = \frac{\rho_s c_{ps} R^2}{k_s} \tag{8}$$

$$\tilde{r} = \frac{r}{R}. \tag{9}$$

The boundary condition (6) can be written as:

$$-\left.\frac{\partial T_s}{\partial r}\right|_{\tilde{r}=1} = \mathrm{Bi}\left(T_s|_{\tilde{r}=1} - T_o\right) \tag{10}$$

where

$$\mathrm{Bi} = \frac{hR}{k_s} \tag{11}$$

is the Biot number.

Take the Laplace Transform of (7). Denote the Laplace transform of T_s by $\Theta(s,\tilde{r})$. Solve the resulting ordinary differential equation to obtain.

$$\tilde{r}\Theta(s,\tilde{r}) = c_1 \cosh(\tilde{r}\sqrt{t_c s}) + c_2 \sinh(\tilde{r}\sqrt{t_c s}) \tag{12}$$

Since the domain is that of a solid sphere, regularity condition excludes singularity at the center of the sphere. That is $c_1 = 0$. Appling the boundary condition (10), we obtain:

$$c_2 = \frac{\mathrm{Bi}\sqrt{t_c s}\,\Theta_o}{(\mathrm{Bi}-1)\sinh\sqrt{t_c s} + \sqrt{t_c s}\cosh\sqrt{t_c s}} \tag{13}$$

Therefore:

$$\Theta(s,\tilde{r}=0) = c_2 \lim_{\tilde{r}\to 0} \frac{\sinh(\tilde{r}\sqrt{t_c s})}{\tilde{r}} = c_2\sqrt{t_c s} \tag{14}$$

Let $\Theta_o(s)$ denote the Laplace transform of the process temperature. Finally, we have

$$\Theta(s,\tilde{r}=0) = G_c(s)\Theta_o(s) \tag{15}$$

where

$$G_c(s) = \frac{\mathrm{Bi}\sqrt{t_c s}}{(\mathrm{Bi}-1)\sinh\sqrt{t_c s} + \sqrt{t_c s}\cosh\sqrt{t_c s}} \tag{16}$$

According to (10), the limit $\mathrm{Bi}\to 0$ corresponds to adiabatic boundary condition on the surface and is not interesting in the context of a temperature sensor. For large Biot number, the temperature on the sphere surface is close to T_o. The corresponding time constant τ approaches zero. In the limit $\mathrm{Bi}\to\infty$, the transfer function for the continuous model becomes:

$$G_c(s) = \frac{\sqrt{t_c s}}{\sinh\sqrt{t_c s}}. \tag{17}$$

Comparing (3), (8), and (11), we get

$$\tau = \frac{\rho_s c_{ps} R}{3h} = \frac{t_c}{3\mathrm{Bi}}. \tag{18}$$

That is

$$t_c = 3\mathrm{Bi}\,\tau. \tag{19}$$

Small Biot number corresponds to fast conduction for which the first order model is accurate. The transfer function $G_c(s)$ determines the steady-state responses to sinusoidal input. Corresponding to sinusoidal process temperature

$$T_o = \sin(\omega t), \tag{20}$$

the steady-state sensor response is given by

$$T_s(r=0) = |G(j\omega)|\sin(\omega t + \phi), \tag{21}$$

that is, a sinusoid with amplitude gain $|G(j\omega)|$ and phase angle $\phi = \angle G(j\omega)$. The frequency response of the continuum model is compared with that corresponding to the first order lag model given below

$$G_1(s) = \frac{1}{\tau s + 1}. \tag{22}$$

Figure 2 shows the gain and the phase angle of the first order lag model and the continuum model with different Biot numbers. Note that the two models are indistinguishable for Biot number less than 0.1. As is well known for the first order system, the gain decreases with the frequency and the phase angle is negative representing the lag. For large Biot number, the temperature on the sphere surface is nearly the same as the process temperature. The conduction within the sphere is determined by a different parameter t_c defined in (8). The phase

lag may exceed π. Namely, the temperature at the center is opposite in phase with the process temperature that sensor is used to measure. This is qualitatively different from the prediction by the first order model for which the maximum phase lag is $\pi/2$.

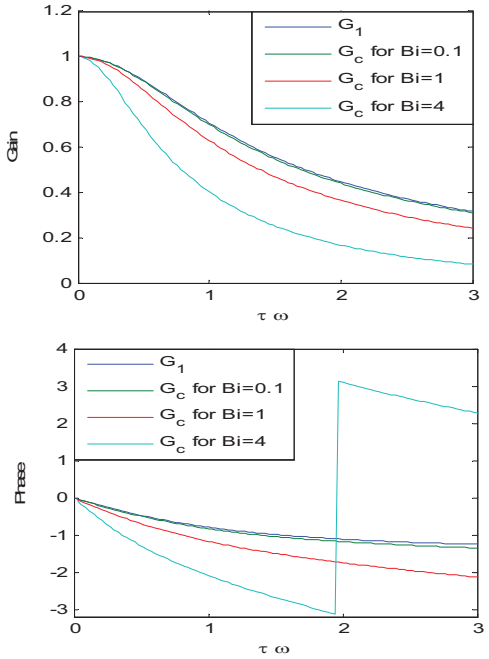

Figure 2. Comparison of the frequency responses of the temperature sensor as given by the first order model (G_1) and the continuum model (G_c) with different Biot numbers.

The purpose of the proposed continuum model is to guide the development of methods for dynamic compensation of temperature sensors. Without dynamic compensation, the sensor has very narrow bandwidth over which the gain is close to one and the phase angle is negligible. In the following section, we first develop numerical solution to the one dimensional heat equation. The numerical solutions will be used in validating the proposed dynamic compensation methods.

III. NUMERICAL SOLUTION USING FINITE DIFFERENCE METHOD

By finite difference method, equation (7) becomes:

$$\frac{t_c \partial T_s^{(i)}}{\partial t} = \frac{1}{\tilde{r}^{(i)}} \frac{\tilde{r}^{(i+1)} T_s^{(i+1)} + \tilde{r}^{(i-1)} T_s^{(i-1)} - 2\tilde{r}^{(i)} T_s^{(i)}}{(\delta\tilde{r})^2}. \quad (23)$$

where $\delta\tilde{r} = 1/(n-1)$. The above equation is valid for i=2, 3, …, n, where the node n lies on the sphere surface. The node i=1 is at the center. For this node, we first write (7) as

$$\frac{t_c \partial T_s}{\partial t} = \frac{2}{\tilde{r}} \frac{\partial T_s}{\partial \tilde{r}} + \frac{\partial^2 T_s}{\partial \tilde{r}^2} \quad (24)$$

Since temperature gradient is zero at the center, we have

$$\frac{t_c \partial T_s^{(1)}}{\partial t} = 2\frac{T_s^{(2)} - T_s^{(1)}}{(\delta\tilde{r})^2}. \quad (25)$$

For node n, we first apply the central differencing to the boundary condition (10) to obtain the temperature at a virtual node $n+1$:

$$T_s^{(n+1)} = T_s^{(n-1)} + 2\mathrm{Bi}(T_o - T_s^{(n)})\delta\tilde{r}. \quad (26)$$

We then use (23) to obtain

$$\frac{t_c \partial T_s^{(n)}}{\partial t} = \frac{1}{\tilde{r}^{(n)}} \frac{\tilde{r}^{(n+1)} T_s^{(n+1)} + \tilde{r}^{(n-1)} T_s^{(n-1)} - 2\tilde{r}^{(n)} T_s^{(n)}}{(\delta\tilde{r})^2}. \quad (27)$$

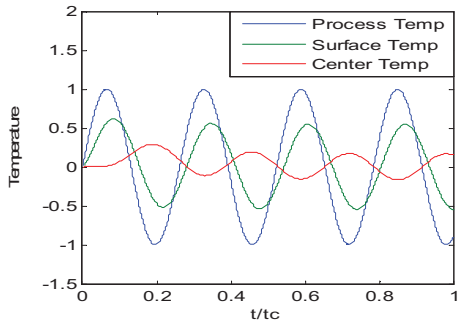

Figure 3 Response to sinusoidal process temperature $T_o = \sin(\omega t)$, where $\tau\omega$=2.0 and Bi=4. The center temperature is opposite in phase with the process temperature.

Equations (25), (23), and (27) represent a system of linear ordinary differential equations. They are solved numerically using standard methods for ordinary differential equations available in Matlab. The numerical solution is rather straightforward. A solution obtained for Bi=4.0 is shown in Figure 3. Corresponding to a sinusoidal process temperature with $\tau\omega$=2.0, the temperature on the sphere surface and at the sphere center quickly converge to sinusoidal functions of the same frequency. Temperatures on the sphere surface and at the center show reduced amplitudes and phase lags. In particular, the temperature at the center is opposite in phase with the process temperature. By carrying out numerical solutions corresponding to different input frequencies, we obtain the steady-state amplitude of the temperature at the sphere center. The obtained amplitude is compared with the gain of the function $|G(j\omega)|$ which is given in (16). Table 1 shows that the agreement is very good for the case with Biot number 1.0. Forty nodes are used in the calculation.

Table 1. Amplitude of the center temperature corresponding to unit amplitude sinusoidal surface temperature. Bi=1.0. 40 nodes are used.

$\tau\omega$	$\lvert G(j\omega)\rvert$ - Theory	$\lvert G(j\omega)\rvert$ - Numerical
0.5	.8522	.8521
1.0	.6284	.6283
1.5	.4694	.4694
2.0	.3646	.3645
2.5	.2929	.2929
3.0	.2413	.2412

IV. DYNAMIC COMPENSATION USING TIME DERIVATIVES OF SENSOR DATA

For the first order lag model, dynamic compensation is accomplished through (2). That is we obtain the process temperature T_o by combining the sensor data T_s and its first order time derivative. With the continuum model, the relationship between the process temperature and the sensor data is given by the non-polynomial transfer function G_c. Through Taylor series expansion, we obtain

$$\frac{1}{G_c(s)} = 1 + (1 + \frac{\mathrm{Bi}}{2})\varpi + \frac{3(4\mathrm{Bi} + \mathrm{Bi}^2)}{40}(\varpi)^2 + \\ + \frac{3(6\mathrm{Bi}^2 + \mathrm{Bi}^3)}{560}(\varpi)^3 + \frac{(8\mathrm{Bi}^3 + \mathrm{Bi}^4)}{4480}(\varpi)^4 + \cdots \quad (28)$$

Using (19), we can express (28) as follows:

$$\frac{1}{G_c(s)} = 1 + \frac{(2+\mathrm{Bi})}{6\mathrm{Bi}} t_c s + \frac{4+\mathrm{Bi}}{120\mathrm{Bi}}(t_c s)^2 + \frac{6+\mathrm{Bi}}{5040\mathrm{Bi}}(t_c s)^3 \\ + \frac{8+\mathrm{Bi}}{362880\mathrm{Bi}}(t_c s)^4 \cdots \quad (29)$$

Therefore, we obtain the following formula for the process temperature from the sensor data in time domain:

$$T_o = \left(1 + \frac{2+\mathrm{Bi}}{6\mathrm{Bi}}\frac{t_c d}{dt} + \frac{4+\mathrm{Bi}}{120\mathrm{Bi}}\frac{t_c^2 d^2}{dt^2} + \frac{6+\mathrm{Bi}}{5040\mathrm{Bi}}\frac{t_c^3 d^3}{dt^3} \right. \\ \left. + \frac{8+\mathrm{Bi}}{362880\mathrm{Bi}}\frac{t_c^4 d^4}{dt^4} + \cdots\right) T_s|_{r=0} \quad (30)$$

In the limit $\tau \to 0$, i.e. $\mathrm{Bi} \to \infty$, (29) becomes

$$\frac{1}{G_c(s)} = 1 + \frac{t_c s}{6} + \frac{(t_c s)^2}{120} + \frac{(t_c s)^3}{5040} + \frac{(t_c s)^4}{362880} + \cdots \quad (31)$$

Equation (30) gives the relationship between the process temperature and the sphere center temperature. It involves time derivatives to infinite order. The practical utility of this equation lies in the approximation with just low order derivatives. The accuracy of the approximations can be obtaining by examining the accuracy of the function (29) by 1st, 2nd, 3rd, 4th approximations in the following:

$$H^{(i)} = 1 + \frac{(2+\mathrm{Bi})}{6\mathrm{Bi}} t_c s; \quad (32)$$

$$H^{(ii)} = H^{(i)} + \frac{4+\mathrm{Bi}}{120\mathrm{Bi}}(t_c s)^2 \quad (33)$$

$$H^{(iii)} = H^{(ii)} + \frac{6+\mathrm{Bi}}{5040\mathrm{Bi}}(t_c s)^3 \quad (34)$$

$$H^{(iv)} = H^{(iii)} + \frac{8+\mathrm{Bi}}{362880\mathrm{Bi}}(t_c s)^4. \quad (35)$$

The comparisons among the above approximations are shown in Figure 4.

The closeness both in amplitude and in phase between the exact function and its approximations is reflected in the accuracy in dynamic compensation using (30). The accuracy improves with the inclusion of successively higher order derivatives. In the following, we use a few terms in (30) to calculate the process temperature using the temperature at the center of the sphere. The center temperature is obtained through numerical solution of the heat equation outlined in the previous section for sinusoidal process temperature. The time derivatives needed in the calculation can be obtained using analog differentiation circuits [24]. From sampled temperature data, we calculate numerical time derivatives using Savitzky-Golay method [25-27]. The Savitzky-Golay method fits sampled data with polynomials of a chosen degree over sub-intervals. The polynomial is determined using least-square method. Time derivatives are calculated from the fitted polynomials. In effect, the time derivatives are obtained through weighted averages of the sampled data. The process temperature, the sensor temperature and the recovered temperature are shown in Figure 5.For the two cases shown in Figure 5, the dynamically compensated temperature using the first order model is close to the process temperature. The first order model appears adequate for these cases with low input frequency. We note that the approximation including third order derivatives is nearly indistinguishable with the process temperature.

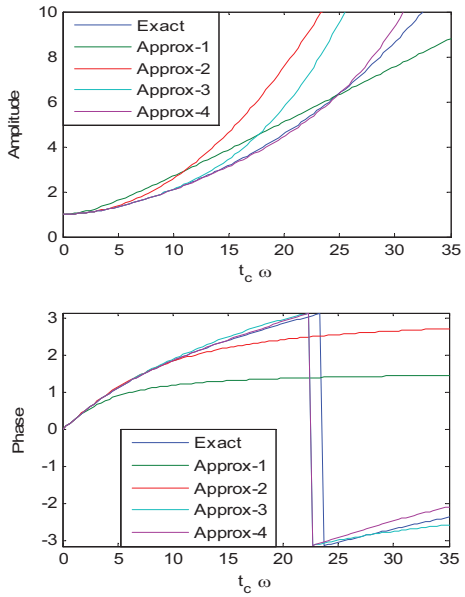

Figure 4. Comparison of low order approximations for Bi=4.

The deviation of the approximation increases with the increasing input frequency. Figure 6 shows the result at higher input frequency, $t_c\omega = 12$. At this frequency, there is a significant phase lag between the center temperature and the process temperature. Note in particular that the first order approximation shows a significant phase lag. As we commented earlier, the maximum phase lag of the first order system is $\pi/2$ which is far different from the phase angle of the exact transfer function. The approximation with third order time derivatives shows excellent agreement except the initial ¼ of the temperature cycle. The larger initial error is due to the non-smoothness of the process temperature T_o as it changes from zero to a sine function. As shown in Figure 7, the initial errors are much smaller for smoother T_o given by

$T_o = 1 - \cos(\omega t)$ which has continuous first order time derivative at $t = 0$.

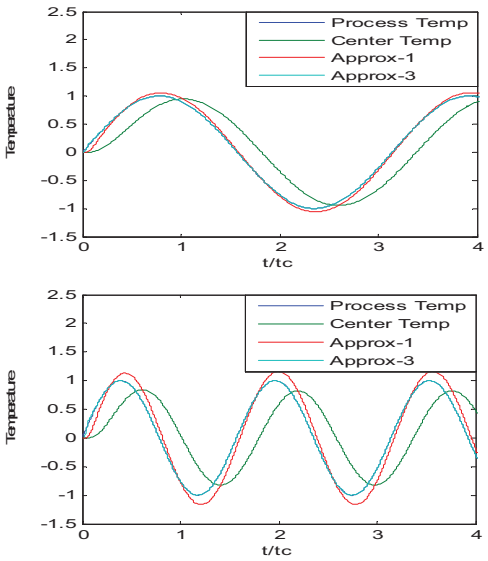

Figure 5. Dynamic compensation including up to third order time derivatives for Bi=4. (a) $t_c\omega = 2$, (b) $t_c\omega = 4$. Note that the curves corresponding to "Process Temp" and "Approx-3" overlap.

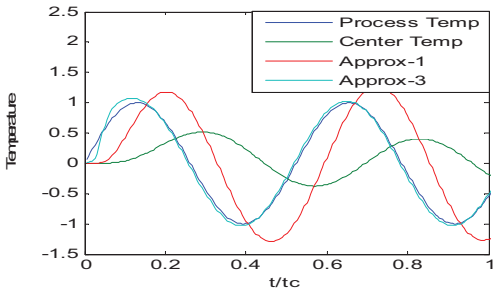

Figure 6 Dynamic compensation including up to third order time derivatives for Bi=4, $t_c\omega = 12$. Note that the curves corresponding to "Process Temp" and "Approx-3" nearly overlap.

Adding higher order time derivatives as given in (29) increases the accuracy of dynamic compensation. Figure 8 shows the comparison for $t_c\omega = 24$. The fourth order approximation and the exact temperature nearly overlap.

Obtaining time derivatives from analog signals requires proper low pass filtering [24]. Otherwise, the output will be saturated by noise. The Savitzky-Golay method has low pass filtering effect since the data points are fitted by polynomial using least-square method. This is especially obvious when one tries to fit many points with a low order polynomial. For example, if we fit five data points by a fourth order polynomial, there is no filtering (or smoothing). On the other hand, if we try to fit more points with the fourth order polynomial, the ripples in the data are smoothed out. We add noise to the center sensor data in the form of αn_i where n_i are pseudorandom numbers following standard normal distribution and α is a scaling coefficient. When seven points are used in the Savitzky-Golay moving averages by a fourth order polynomial, we found that higher order time derivatives are dominated by noise. The result when $\alpha = 2.0 \times 10^{-5}$ is shown in Figure 9. The recovered temperature is barely acceptable for unrealistically small noise level. When 29 points are used, however, dynamic compensation is seen to work well for a reasonable size of noise with $\alpha = 0.01$ as shown in Figure 10.

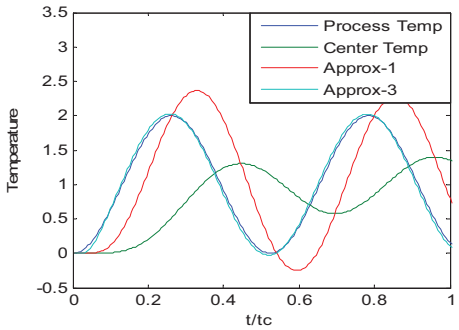

Figure 7. Improvement in Approx-3 for $T_o = 1 - \cos(\omega t)$ and $t_c\omega = 12$. Bi=4. The first order time derivative of T_o is continuous at $t = 0$.

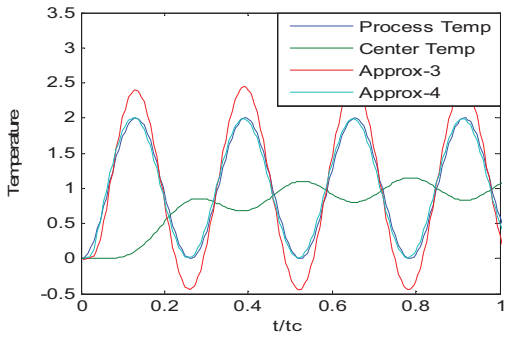

Figure 8. Comparison among the exact temperature and the third and fourth order approximations for $t_c\omega = 24$, Bi=4.

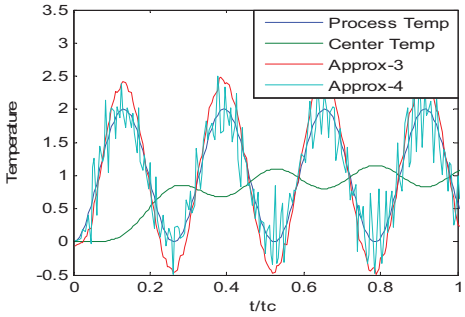

Figure 9. Dynamic compensation when sensor data is contaminated by noise: $t_c\omega = 24$. Bi=4, α =2e-5. Seven points are fitted by a fourth order polynomial.

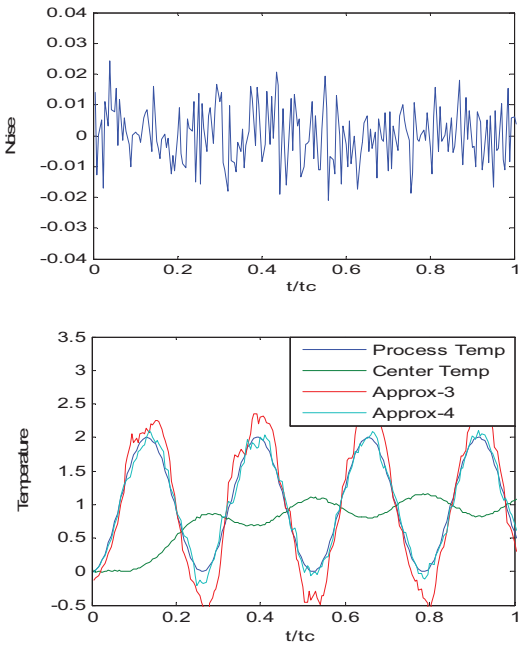

Figure 10. Dynamic compensation when sensor data is contaminated by noise: $t_c\omega = 24$. Bi=4, α =0.01. Twenty nine points are fitted by a fourth order polynomial.

V. DYNAMIC COMPENSATION OF RANDOM SENSOR INPUT WITH NOISE

We have conducted the dynamic compensation for random process temperature. The sensor data we use are obtained from numerical simulations corresponding to random process temperature. The Band-Limited White Noise block in Simulink generates normally distributed random numbers that are suitable for use in continuous or hybrid systems. The white noise is filtered by a second order analog filter with the transfer function given by

$$H(s) = \frac{\omega_n^2}{s^2 + 2\varsigma\omega_n s + \omega_n^2} \tag{36}$$

with $\varsigma = 0.707$ and $\omega_n = 4\pi / t_c$. The low pass filtered signal is used as the process temperature in the numerical simulation outlined in section 3.

Figure 11 shows the result of dynamic compensation obtained using 19 points and 4th order polynomial in Savitzky-Golay numerical differentiation. Sampling interval is $0.005\,t_c$. Note that the fourth order approximation and the process temperature nearly overlap. Moreover, the temperature obtained from dynamic compensation shows much more dynamic fluctuations from the center temperature.

As demonstrated in the above section, sensor noise can present difficulty in obtain numerical derivatives. For the identical random input as in Figure 11, a random noise with α =0.01 is added to the center temperature. Figure 12(a) shows the large fluctuations in the reconstructed temperature. Nevertheless, when 29 points are used in Savitzky-Golay, the recovered temperature appears acceptable except near the very end. In practice, we can obtain extra samples beyond the time interval of interest and use them for the dynamic compensation.

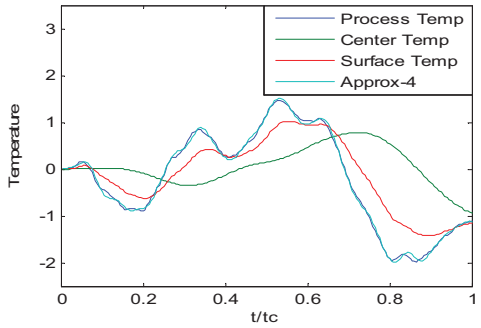

Figure 11, Dynamic compensation for random process temperature. Nineteen points are used in Savitzky-Golay numerical differentiation. Bi=4.

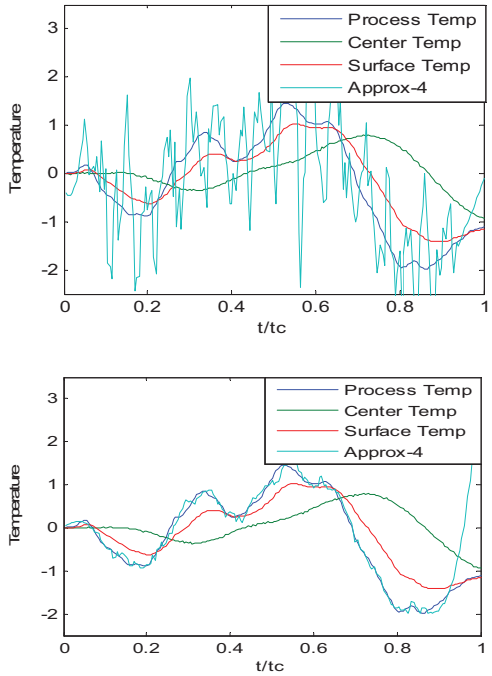

Figure 12. Dynamics compensation in the presence of sensor noise α =0.01, Bi=4. (a) 19 points in Savitzky-Golay; (b)29 points in Savitzky-Golay.

VI. CONCLUSIONS

We have presented a continuum model for temperature sensor. This model is used to obtain dynamic compensation of the sensor to enable it for measurement of dynamic signals of much broader bandwidth. If we are able to significantly broaden the bandwidth of temperature sensors, it may be possible to use

them for new sensing applications such as proximity detection, flow measurement, and motion sensing.

REFERENCES

1. M. Nabavi, Unsteady and pulsating pressure and temperature: a review of experimental techniques. Review of Scientific Instruments, Vol. 81, 031101, 2010.
2. M.E. Bourg, W.E. van der Veer, A.G. Grüell, and R.M. Penner, Electrodeposited submicron thermocouples with microsecond response times, Nano Letters, Vol. 7 (10), 3208-3213, 2007.
3. T.E. Diller, W.W. Robinson, and W.B. Watkins, Dynamic gas temperature measurement system, NASA CR-168267, 1983.
4. Z. Yang, and X. Meng, Research on the dynamic calibration of thermocouple and temperature excitation signal generation method based on shock-tube theory, Journal of Engineering for Gas Turbines and Power, Vol. 136, 071602 (10 pages), 2014.
5. P.G. O'Reilly, R.J. Kee, R. Fleck, and P.T. McEntee, Two-wire thermocouples: a nonlinear state estimation approach to temperature reconstruction, Review of Scientific Instruments, Vol. 72 (8), 3449-3457, 2001.
6. K. Kar, S. Roberts, R. Stone, M. Oldfield, and B. French, Instantaneous exhaust temperature measurements using thermocouple compensation techniques, SAE Technical Paper 2004-01-1418, 2004. doi:10.4271/2004-01-1418.
7. L. Qingyang, Z. Yuanliang, and X. Wei, Dynamic compensation of Pt100 temperature sensor in petroleum products testing based on a third order model," IEEE International Workshop on Intelligent Systems and Applications (IEEE, 2009), May 23-24, Wuhan, China, pp. 1-4, 2009.
8. R. Zimmerschied and R. Isermann, Nonlinear time constant estimation and dynamic compensation of temperature sensors, Control Engineering Practice, vol. 18, 300-310, 2010.
9. S. Yao and R. Gao, Nonlinear dynamic compensation research on temperature measurement system in coal mine movable refuge chamber, Procedia Engineering, vol. 26, 2306-2312, 2011.
10. Y. Wang and J. Yin, The research of a new type of sensor dynamic compensation, Procedia Engineering, Vol. 15, 1575-1579, 2011.
11. F. Yan and J. Wang, Pressure-based transient intake manifold temperature reconstruction in diesel engines, Control Engineering Practice, vol. 20, 531-538, 2012.
12. K. Tomczuk and R. Werszko, Correction for thermal lag in dynamic temperature measurements using resistance thermometers, Review of Scientific Instruments, vol. 84, 074903-1 (7 pages), 2013.
13. Y. Liu, S. Liu, Z. Qin, Z. Zhang, and L. Meng, Dynamic compensation of sensors based on improved recursive least squares algorithm, Proceedings of 2013 IEEE International Conference on Mechatronics and Automation, August 4-7, Takamatsu, Japan, 196-200, 2013.
14. C.E. Shepard and I. Warshawsky, Electrical techniques for compensation of thermal time lag of thermocouples and resistance thermometer elements, NACA Tech Note 2703, 1952.
15. T.W. Kerlin, H.M. Hashemian, and K.M. Peterson, Time Response of Temperature Sensors, ISA Trans., vol. 20, no.1, 65-77. 1981.
16. M. Tagawa, T. Shimoji, and Y. Ohta, A two-thermocouple probe technique for estimating thermocouple time constants in flows with combustion: In situ parameter identification of a first-order lag system, Review of Scientific Instruments, vol. 69, no. 9, 3370-3378, 1998.
17. M Tagawa, K. Kato, and Y. Ohta, Response compensation of temperature sensors: frequency-domain estimation of thermal time constants, Review of Scientific Instruments, vol. 74, no. 6, 3171-3174, 2003.
18. M. Tagawa, K. Kaifuku, T. Houra, Y. Yamagami, and K. Kato, Response compensation of fine-wire thermocouples and its application to multidimensional measurement of a fluctuating temperature field, Heat Transfer-Asian Research, vol. 40 (5), 404-418, 2011.
19. S.M. Khine, T. Houra, and M. Tagawa, An adaptive response compensation technique for the constant-current hot-wire anemometer, Open Journal of Fluid Dynamics, vol. 3, 95-108, 2013.
20. C.J. Kobus, True fluid temperature reconstruction compensating for conduction error in the temperature measurement of steady fluid flows, Review of Scientific Instruments, vol. 77, 034903 (10 pages), 2006.
21. K. Kato, M. Tagawa, and K. Kaifuku, Fluctuating temperature measurement by a fine-wire thermocouple probe: influences of physical properties and insulation coating on the frequency response. Measurement Science and Technology, vol. 18, 779-789, 2007.
22. M. Tagawa, K. Kato, and Y. Ohta, Response compensation of fine-wire temperature sensors, Review of Scientific Instruments, vol. 76, 094904 (10 pages), 2005.
23. S.M. Khine, T. Houra, and M. Tagawa, Heat-conduction error of temperature sensors in a fluid flow with nonuniform and unsteady temperature distribution, Review of Scientific Instruments, vol. 84, 044902 (11 pages), 2013.
24. B.S. Elkins, M. Huang, J. Frankel, Higher-time derivative of in-depth temperature sensors for aerospace heat transfer, International Journal of Thermal Sciences 2012; 52:31-39.
25. A. Savitzky and M.J.E. Golay, Smoothing and differentiation of data by simplified least squares procedures, Anal. Chem. 36 (1964), 1627-1639.
26. P.A. Gorry, General least-squares smoothing and differentiation by the convolution (Savitzky-Golay) method, Anal Chem. 62 (1990), 570-573.
27. Z. C. Feng, J. K. Chen, Y. Zhang, S. Montgomery-Smith, Temperature and heat flux estimation from sampled transient sensor measurements, Int. J. of Thermal Sciences 49 (2010) 2385-2390.